

## The WFCAM multiwavelength Variable Star Catalog (Corrigendum)

C. E. Ferreira Lopes<sup>1</sup>, I. Dékány<sup>2,3</sup>, M. Catelan<sup>2,3</sup>, N. J. G. Cross<sup>4</sup>, R. Angeloni<sup>5</sup>, I. C. Leão<sup>1</sup>, and J. R. De Medeiros<sup>1</sup>

<sup>1</sup> Departamento de Física Teórica e Experimental, Universidade Federal do Rio Grande do Norte, 59072-970 Natal, RN, Brazil  
 e-mail: ferreiralopes1011@gmail.com

<sup>2</sup> Instituto de Astrofísica, Pontificia Universidad Católica de Chile, Av. Vicuña Mackenna 4860, 782-0436 Macul, Santiago, Chile

<sup>3</sup> Millennium Institute of Astrophysics, Santiago, Chile

<sup>4</sup> SUPA (Scottish Universities Physics Alliance) Wide-Field Astronomy Unit, Institute for Astronomy, School of Physics and Astronomy, University of Edinburgh, Royal Observatory, Blackford Hill, Edinburgh EH9 3HJ, UK

<sup>5</sup> Gemini Observatory, Colina El Pino, Casilla 603, La Serena, Chile

A&A 573, A100 (2015), DOI: 10.1051/0004-6361/201423793

**Key words.** stars: variables: general – infrared: stars – dust, extinction – stars: formation – techniques: photometric – errata, addenda

The multiplicative expression on the  $I_{\text{pfc}}^{(s)}$  (see Sect. 3.1, Eq. (6)) variability indices does not properly correct for different numbers of epochs in different filters. The expression can be written in the following form:

$$\sqrt{\frac{(n_s - s)!}{n_s!}} = \sqrt{\frac{1}{\prod_{j=1}^{s-2} [n_s - (s - j)]}} \cdot \sqrt{\frac{n_s}{(n_s - 1)}} \cdot \frac{1}{n_s}, \quad (1)$$

where  $s > j$ .  $\sqrt{n_s/(n_s - 1)}$  is the Bessel correction while  $1/n_s$  is the factor for the mean value. The first parameter (right side) is incorrect and introduces a bias related to  $n_s$  values when  $s > 2$ . Additionally the Bessel correction needs to be repeated for each additional correlation term, as we show below. Indeed, the weight of this bias must increase with both  $s$  and  $n_s$ . Therefore these indices must be replaced by following,

$$I_{\text{pfc}}^{(s')} = \frac{1}{n_s} \sum_{i=1}^n \left[ \sum_{j_1=1}^{m-(s-1)} \cdots \left( \sum_{j_s=j_{(s-1)}+1}^m \Lambda_{ij_1 \dots j_s}^{(s)} \sqrt{\Gamma u_{ij_1} \cdots \Gamma u_{ij_s}} \right) \right], \quad (2)$$

where  $\Gamma$  is given by,

$$\Gamma u_{ij} = \sqrt{\frac{n_{u_{j_s}}}{n_{u_{j_s}} - 1}} \times \left( \frac{u_{ij_s} - \bar{u}_{j_s}}{\sigma_{u_{j_s}}} \right), \quad (3)$$

where  $u_{ij_s}$  is the  $i$ th epoch of filter  $j_s$ . This new index is the mean value of the correlations and it is not biased for  $n_s$ ; additionally it reduces to  $I_{\text{pfc}}^{(s')} = J_{\text{WS}}$  for  $s = 2$ .

As discussed above, the analysis of  $I_{\text{pfc}}^{(s)}$  for  $s > 2$  in Fig. 5 is incorrect since the index is biased by the extra first term such that the index is relatively reduced in value at larger values of  $n_s$ . A corrected version is shown in Fig. 1, which shows the distribution of the unbiased variability indices ( $I_{\text{pfc}}^{(s')}$ ) as a function of  $K$  magnitude. These  $I_{\text{pfc}}^{(s')}$  indices present a similar range of values for different values of  $s$ . Additionally, we can observe that the centre of the distribution ( $m$ ) decreases with increasing  $s$ , whilst the full-width at half maximum increases. This is caused

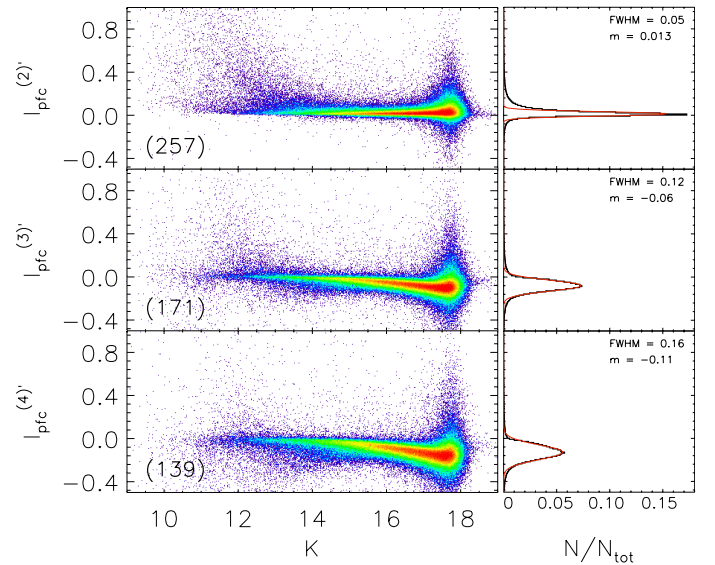


**Fig. 1.**  $I_{\text{pfc}}^{(s')}$  variability indices versus the  $K$ -band magnitude for the initial database, for three values of  $s$ :  $s = 2$  (upper panel),  $s = 3$  (middle panel), and  $s = 4$  (lower panel) on the left-hand side, with histograms of each distribution on the right-hand side. The red line marks a Gaussian fit and we record the full-width half maximum and centre in each right-hand panel.

by an asymmetry in the number of combinations that produce negative values compared to positive values with increasing  $s$ . Real correlated variations return positive values, whereas random or semi-correlated noise is much more likely to return negative values. This leads to a better discrimination between variable and non-variable stars as  $s$  increases. For instance, we can select about 90% of the WFCAM Variable Stars Catalog in a sample 2.2 times smaller when  $s = 4$  than that when  $s = 2$ .

The shape of the cut-off surfaces in Fig. 6 for  $I_{\text{pfc}}^{(3)}$  is unbiased in the magnitude dimension, but the  $n_s$  dimension is biased by  $\sqrt{1/(n_s - 2)}$ . The selections of variable star candidates were

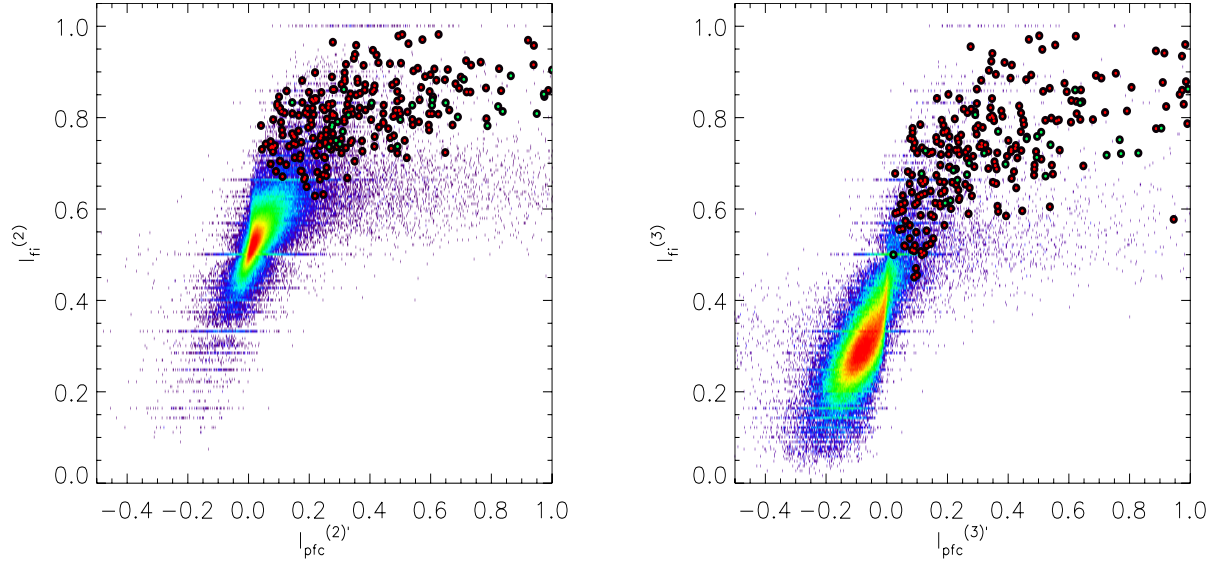


**Fig. 2.** Distribution of  $I_{fi}^{(s)}$  versus  $I_{pfc}^{(s)'$  variability indices, for orders 2 (*left*) and 3 (*right*). The C1 and C2 sources are indicated by red and green circles, respectively.

performed for  $I_{pfc}^{(s)}$  as well as  $I_{fi}^{(s)}$ .  $I_{pfc}^{(2)}$  and  $I_{fi}^{(s)}$  are unbiased and they may provide a complete selection of variable stars candidates. Meanwhile, the incorrect factor in  $I_{pfc}^{(s)}$  for  $s > 2$  does not provide a strong bias in our selection because the selection is performed using the cut-off surfaces which are modified to take the mean effect of the bias into account. However,  $I_{pfc}^{(s)}$  indices

should be replaced by  $I_{pfc}^{(s)'}$  indices, since the surfaces can correct for the average bias factor but there is an increased variance in  $I_{pfc}^{(s)}$  that could be reduced by using  $I_{pfc}^{(s)'}$ .

Figure 2 shows the corrected plot of panchromatic variability indices  $I_{pfc}^{(s)}$  versus flux independent  $I_{fi}^{(s)}$  (see Fig. 8). As expected, the overlap at large values of  $I_{fi}^{(s)}$  remains.